

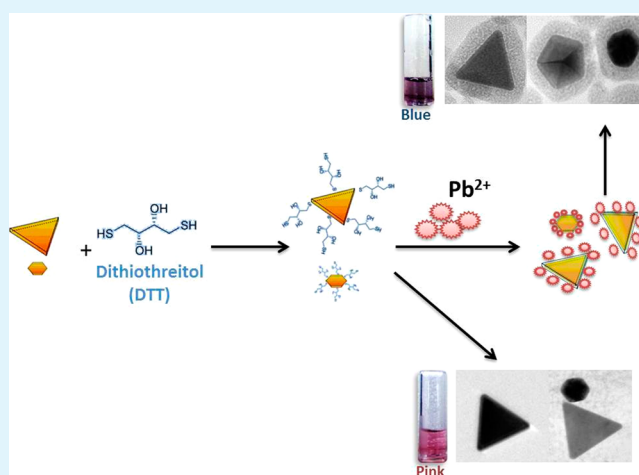
# Direct Visualization of Lead Corona and Its Nanomolar Colorimetric Detection Using Anisotropic Gold Nanoparticles

Charu Dwivedi,\* Abhishek Chaudhary, Abhishek Gupta, and Chayan K. Nandi\*

School of Basic Sciences, Indian Institute of Technology Mandi, Mandi-175001, India

## S Supporting Information

**ABSTRACT:** The study presents dithiothreitol (DTT) functionalized anisotropic gold nanoparticles (GNP) based colorimetric sensor for detection of toxic lead ions in water. Our results demonstrate the selectivity and sensitivity of the developed sensor over various heavy metal ions with detection limit of  $\sim 9$  nM. The mechanism of sensing is explained on the basis of unique corona formation around the DTT functionalized anisotropic GNP.



**KEYWORDS:** anisotropy, gold nanoparticles, lead ions, colorimetric assay, corona formation

Lead ion creates a great threat to the health of living beings and the environment worldwide. Lead contaminates water and soil, and ultimately enters in the food chain. Gradual accumulation of lead in central nervous and endocrine systems causes serious diseases especially in infants and toddlers.<sup>1–3</sup> Its exposure is estimated to account for 143 000 deaths per year with the highest burden in developing regions.<sup>4–6</sup> Thus, it is quite imperative to develop suitable  $\text{Pb}^{2+}$  detection systems with high sensitivity and reliability. In the past decades various colorimetric and fluorometric detection systems based on biomolecules, nanoparticles, fluorophors, polymers etc., have been proposed for detection of lead ions in contaminated water.<sup>7–10</sup> Particularly colorimetric assays have attracted considerable attention for toxic metal ion detection because of their simplicity, low cost and on-site application for environmental monitoring.<sup>11–13</sup> Among several metal nanoparticles, gold nanoparticles have received great attention in the development of visual sensing schemes because of the surface plasmon resonance (SPR) which is extremely sensitive to their nature, size, shape, their interparticle distances, and the nature of their surrounding media.<sup>14</sup> Chai et al., have reported spherical GNP and glutathione based colorimetric sensor for lead detection with detection limit (DL) 100 nM.<sup>15</sup> Gua et al. have demonstrated application of peptide functionalized GNP in detection of lead ion with DL 200 nM.<sup>16</sup> The selectivity for lead ion can be achieved by using specific chemicals but the detection limit of these chemical-based sensors is lower than the U.S. Environmental Protection Agency (EPA) permitted

maximum  $\text{Pb}^{2+}$  value (72 nM) in drinking water.<sup>17</sup> Recently, a series of functional DNAzyme-based sensors by using GNPs have been demonstrated by Lu and co-workers. The detection range of these sensors could be tuned from 3 nM to 1  $\mu\text{M}$ .<sup>18,19</sup> Wei and co-workers reported a DNAzyme-based colorimetric sensor for  $\text{Pb}^{2+}$ , the detection limit was 500 nM.<sup>20</sup> Although, these sensors have shown quite high selectivity and sensitivity, but these systems involve complex synthetic procedure. Moreover, the DNA oligomers used are quite expensive and need specific sample pretreatment which limits their applications for many real samples. Recent advances in shape controlled synthesis of metallic nanoparticles of different size and the ability to tailor their surface chemistry by introducing suitable surface modifiers have opened new opportunities to detect metal ions in selectively even in the nanomolar range.<sup>21–24</sup> Here, we report a new strategy to use anisotropic GNP surface functionalized with dithiothreitol (DTT) for detection of lead ions in nanomolar to micromolar range. The gold nanoparticles used are of triangular plate and hexagonal in shape. To ascertain the role of anisotropy in the colorimetric sensing, we carried out the comparative studies with DTT functionalized spherical GNP.

Anisotropic GNP and spherical GNP were prepared using a seed-mediated growth method in the presence of cetyltri-

**Received:** October 28, 2014

**Accepted:** February 26, 2015

**Published:** February 26, 2015



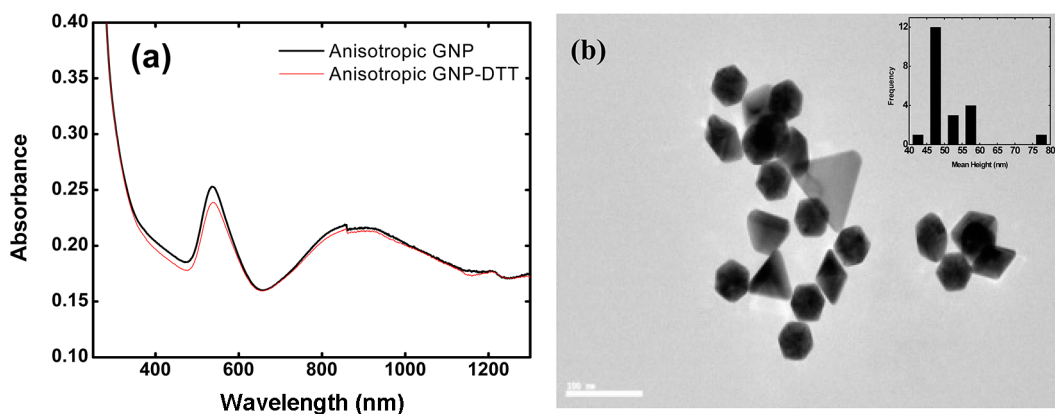
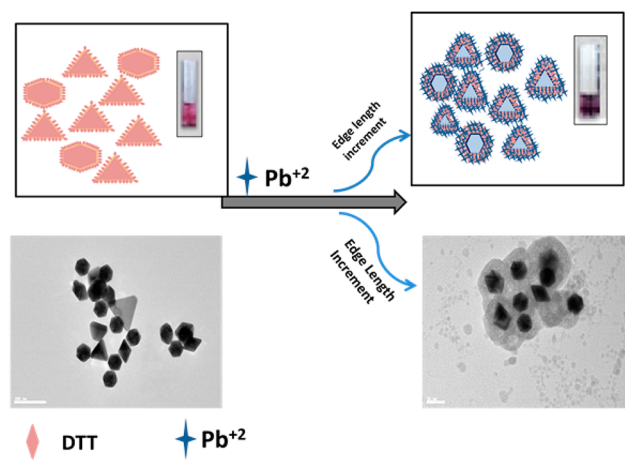


**Figure 1.** (a) UV–vis–NIR spectra of anisotropic GNP and DTT functionalized anisotropic GNP. (b) TEM image of anisotropic GNP and inset shows the corresponding size distribution histogram.

thylammonium bromide (CTAB) (Figure S1a in the Supporting Information).<sup>25</sup> The surface functionalization of the nanoparticles was carried out with an optimized concentration of DTT (Figure S1b in the Supporting Information). Figure 1a depicts the absorption spectrum acquired from the anisotropic GNP and DTT functionalized anisotropic GNP suspension in the visible–NIR range. The band with  $\lambda_{\text{max}}$  at 536 nm is associated with out-of-plane SPR because of the hexagonal and triangular plate nanoparticles. A second band is observed at 880 nm, assigned to the in-plane quadrupole mode of the anisotropic GNP. The band is broad because of the relatively high polydispersity, both in size and shape, which implies quite a broad range of possible resonance frequencies.<sup>26</sup> In addition to this a SPR band of relatively low intensity is observed at 1211 nm, which is assigned to dipole resonance of the triangular gold nanoparticles. The transmission electron microscopy (TEM) image of the anisotropic GNP indicates that their average size is  $\sim 47$  nm (Figure 1(b)). After surface functionalization a red shift of 2 nm is observed in the band at 536 nm was observed, however the peak position of the second band at 880 nm remains unaltered. Although a small decrement in the absorption intensity is observed in both the SPR bands after surface functionalization with DTT indicating change in local environment around anisotropic GNP. Zeta potential of the nanoparticles was also measured before and after surface functionalization. A huge decrement of 67 mV is observed in the zeta potential of the DTT functionalized anisotropic GNP as compared to that of the CTAB-coated anisotropic GNP. The change in zeta potential is related to the change in electrokinetic charge at the nanoparticles. As evident from Figure S2 in the Supporting Information, the surface charge on the as prepared CTAB-coated anisotropic gold nanoparticles is considerably decreased after surface modification. UV–vis–NIR spectrophotometric data and zeta potential results indicate good replacement of CTAB molecules and successful coverage of the nanoparticles with DTT.

The principle of the assay is proposed in Scheme 1. Because the active sites on the anisotropic GNP are their corners and edges, due to their preferential functionalization, the binding of lead ions and the resulting corona formation is more efficient on these facets. The polymeric complexation of the lead ions on these sites results in red shift in the SPR bands and the color change. In the absence of  $\text{Pb}^{2+}$  or in the presence of other metal ions, however, no polymeric complexation should occur, and

### Scheme 1. Schematic Illustration Showing the Mechanism of Lead Ion Detection by DTT Functionalized Anisotropic GNP via Corona Formation



the size of the anisotropic GNP remains the same and hence no color change is observed.

To establish the true potential of the developed sensor, we optimized the detection conditions for the sensor by varying the concentration of anisotropic GNP and the time of equilibration. Initial analysis was conducted by UV–visible–NIR spectroscopy, which is highly sensitive to the change in local environment of nanoparticles discernible from the red-shift in the plasmon peak. Change in absorption intensity at 538 and 880 nm, for different concentrations of DTT functionalized anisotropic GNP, were monitored at different time intervals. It was observed that  $\sim 10$  min of time is sufficient to induce significant color change and red shift in the absorption spectra of the sensing system and no major change is observed after 30 min of equilibration (Figure S3a, b, Supporting Information). Because the color change is more pronounced at higher concentration of anisotropic GNP (50 nM) within 10 min of contact time, therefore, we carried out all the experiments under these optimized conditions of concentration and contact time. Figure 2a depicts the absorption spectra of the anisotropic GNP system after the addition of lead ion (500 nM). A red shift of 5 and 30 nm is observed in the band at 538 and 880 nm, respectively, after 10 min of contact time. This huge shift and broadening of the band at 880 nm could be due to the binding of lead ions with

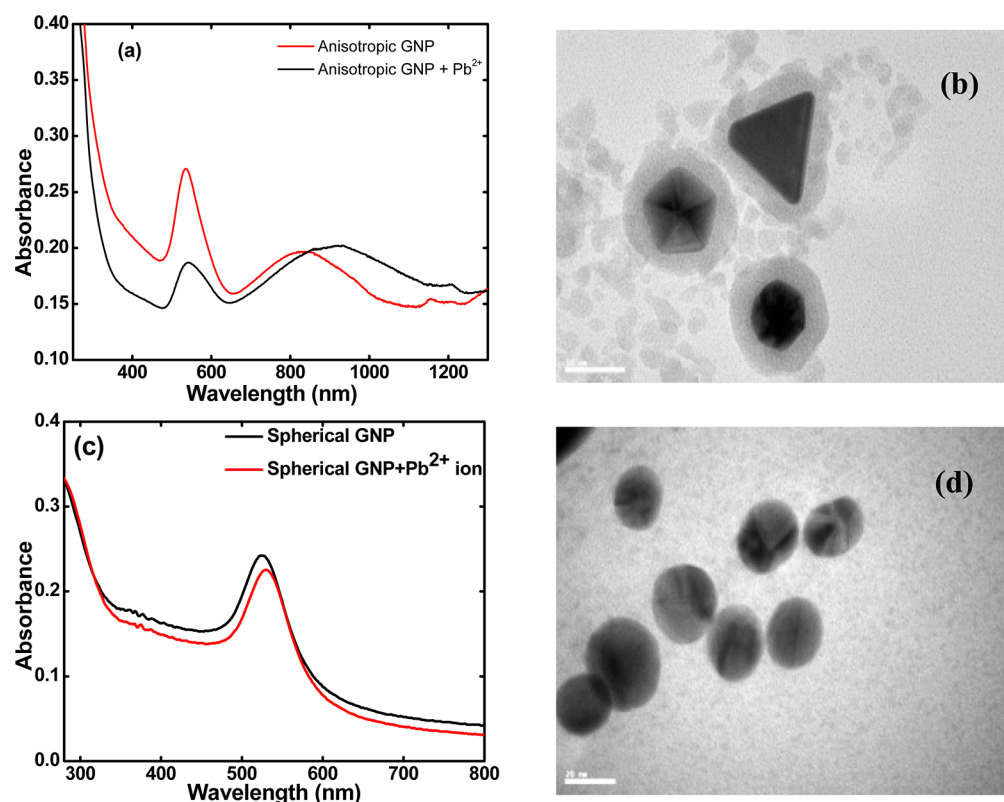


**Figure 2.** (a, c) UV-vis-NIR spectra of DTT functionalized anisotropic GNP and spherical GNP, respectively, before and after addition of lead ions (500 nM) (b, d) TEM image of DTT functionalized anisotropic GNP and spherical GNP, respectively, after the addition of lead ions.

DTT in polymeric fashion onto the surface of anisotropic GNP, which results in the increase in size of the nanoparticles. This is also evident from the TEM image, which shows that a corona of thickness of  $\sim 18$  nm is formed around the anisotropic GNP (Figure 2b). The gradual increase in the size of DTT functionalized anisotropic GNP was also monitored by measuring their hydrodynamic radius with respect to time. The size of DTT functionalized anisotropic GNP is observed to be increased by 21 nm within 10 min of contact time and thereafter no significant change in size is observed (see Figure S4 in the Supporting Information).

The sensing in this system is based on the anisotropic GNP surface functionalized with dithiothreitol. DTT is commonly used in biochemical research to protect sulfhydryl groups from oxidation or reduce disulfide linkages to free sulfhydryl groups in proteins and enzymes. DTT is also a strong chelating reagent. The presence of two thiol groups allows it to form specific and very stable polymeric complexes with divalent tetrahedral lead ions.<sup>27</sup> This unique property of DTT is exploited here to detect lead ions, and the role of the gold nanoparticles is to provide the surface for binding and act as color changing probe. It is reported that the (111) facet of hexagonal and triangular plate GNP are of low energy and hence the surface functionalization will be preferred on the same facet.<sup>28,29</sup> Here also the preoriented functionalization is increasing the local concentration of DTT molecule on these planes. On addition of Pb<sup>2+</sup>, a polymeric complex is formed in between Pb<sup>2+</sup> and DTT on the surface of anisotropic GNP as well as present in the solution. This results in the formation of a layer/corona around anisotropic GNP (Figure 2b). This corona around anisotropic GNP increases their edge length and a red shift is observed in the band at NIR region.<sup>29</sup> The resulting

increase in the size of the nanoparticles is also responsible for pink to blue color transition of the solution and hence the colorimetric sensing of the lead ions. The consecutive coverage of the (111) facet increases the roughness of the surface of anisotropic GNP and hence the surface energy of the nanoparticles also increases which ultimately results in their agglomeration (Figure S5, Supporting Information). The complete precipitation of anisotropic GNP in the presence of Pb<sup>2+</sup> is observed within 4 h.

To establish the importance of anisotropy in sensing action, DTT functionalized spherical gold nanoparticles were equilibrated with 500 nM of Pb<sup>2+</sup> ions for 1 h and the changes in the absorption maxima were recorded using UV-vis spectrophotometer (Figure S6a, b, Supporting Information). A slight decrease in the absorption intensity and red shift of only 4 nm, in the SPR band of spherical GNP at 526 nm was observed with no visible change in the color (Figure 2c). TEM analysis of the same sample was also carried out to visualize the change occurring on the surface of the spherical gold nanoparticles. As it is evident from Figure 2d, unlike DTT functionalized anisotropic GNP system, no corona formation is observed in the DTT-spherical GNP system. The spherical GNP are not able to undergo preferential surface functionalization at certain sites because of its isotropic nature and hence the extent of the ligand coverage is also less as compared to the anisotropic particles.<sup>30</sup> This proves that anisotropic surface of the GNP provides higher localized concentration of DTT, which initiates the polymerization binding of DTT resulting in corona formation and the respective color change.

The sensitivity of the sensor was quantitatively evaluated by treating DTT functionalized anisotropic GNP with various concentrations (1–1000 nM) of lead ions, (Figure S7a,

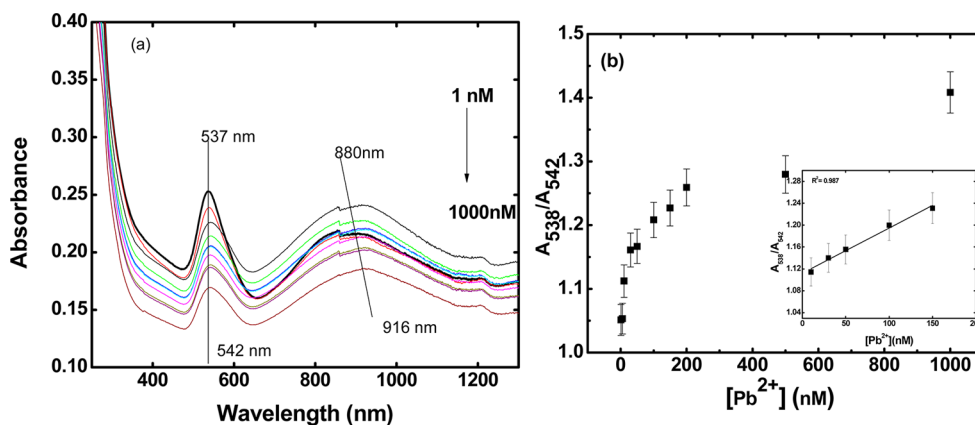


**Figure 3.** (a) UV-vis-NIR spectra of DTT functionalized anisotropic GNP equilibrated for 10 min, with different concentrations of lead ions (1–1000 nM) (b) change in absorption intensity at 538 nm with change in concentration of lead ions, each data point is presented as standard deviation from three replicate assays.

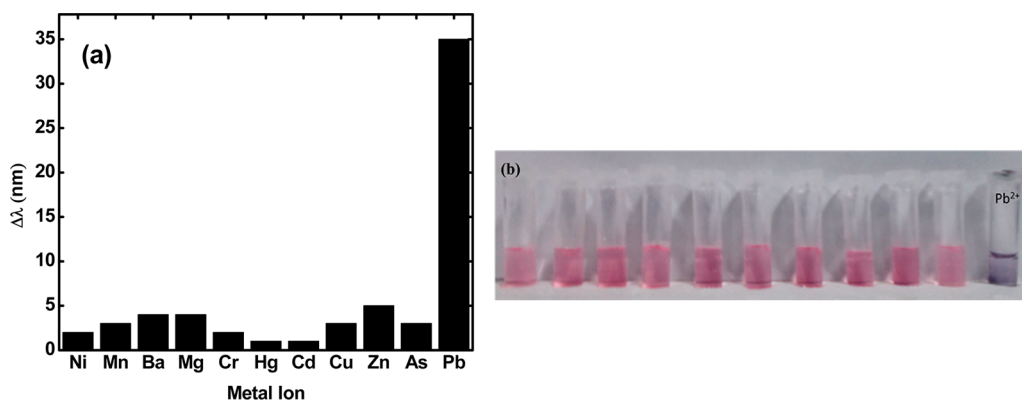


**Figure 4.** (a) Peak shifts in the SPR band of DTT functionalized anisotropic GNP at 880 nm in the presence of different metal ions (b) DTT functionalized anisotropic GNP solutions in the presence of different metal ions (in left to right order, Ni<sup>2+</sup>, Mn<sup>2+</sup>, Ba<sup>2+</sup>, Mg<sup>2+</sup>, Cr<sup>3+</sup>, Hg<sup>2+</sup>, Cd<sup>2+</sup>, Cu<sup>2+</sup>, Zn<sup>2+</sup>, As<sup>3+</sup>, Pb<sup>2+</sup>; [M<sup>n+</sup>] = 500 nM).

Supporting Information). The addition of lead ions into the functionalized anisotropic GNP resulted in the considerable red shift in their surface plasmon bands. Figure 3a shows the change in the absorption intensity of the functionalized anisotropic GNP at various lead ion concentrations. A decrease in the absorption intensity is observed with increase in the lead ion concentration. These experiments show that this technique can detect lead ions in nano molar range within 10 min of equilibration time (Figure S7b, Supporting Information). The extinction ratio between 538 and 542 nm was compared at different lead concentrations to calculate the detection limit (Figure 3b). From the slope of the linear plot (inset Figure 3b), the detection limit was estimated to be 8.9 nM at a signal-to-noise (S/N) ratio of 3, which is even lower than that for most of the chemical based GNP sensors for lead and the maximum contamination limit for lead ions (72 nM) defined by EPA. The SPR at 538 nm was chosen for the calculation of DL, as it is not only the major SPR peak for hexagonal nanoparticles but also has significant contribution from triangular plate nanoparticles. The DL for the system was also determined by calibrating SPR shift ( $\Delta\lambda$ ) at 880 nm with change in lead ion concentration and was found to be 7.6 nM, which is in close agreement with the same determined from SPR at 538 nm (Figure S8, Supporting Information).

To examine the selectivity of the sensor for lead ions, we equilibrated DTT functionalized anisotropic GNP with 500 nM

solution of Cd<sup>2+</sup>, Cu<sup>2+</sup>, Hg<sup>2+</sup>, Zn<sup>2+</sup>, Ni<sup>2+</sup>, Cr<sup>3+</sup>, Ba<sup>2+</sup>, Ca<sup>2+</sup>, Mg<sup>2+</sup>, and As<sup>3+</sup> ions and monitored the change in the SPR band of the nanoparticles and color change. However, no significant changes in the SPR band as well as the color of the nanoparticles were observed even at such higher concentrations of metal ions, except slight red shift in the absorption intensity at 880 nm in all the cases (Figure 4a, b). This could be due to the metal ions possibly being deposited on the surface of gold nanoparticles and changing the SPR of the same. But only lead ions are capable of forming polymeric complex with DTT onto the surface of anisotropic GNP and inducing color change. The time and the nature of response of these other metal ions did not match with that of lead ions, which makes the system selective for lead ion detection.

The applicability of the developed colorimetric assay to real samples was evaluated by spiking tap water (sampled from Mandi, India; see Supporting Information, Table S1, for ion composition of the tap water) with Pb<sup>2+</sup>. Figure S9, Supporting Information, shows the response of the colorimetric assay to tap water samples with Pb<sup>2+</sup> concentrations of 1–1000 nM. The response of the sensor in deionized water and tap water are very similar suggesting that the developed colorimetric sensor can detect Pb<sup>2+</sup> even in the interfering matrix of the tap water. The DL for Pb<sup>2+</sup> in tap water experiments were determined to be 15.9 nM (S/N = 3). Although, a slight decrease in the response of the assay in real sample is observed, still the DL is

much below the allowed  $\text{Pb}^{2+}$  concentration (72 nM) as mentioned earlier.

In conclusion, we have demonstrated a surface modified colorimetric sensor using triangular plate and hexagonal gold nanoparticles that can detect lead ions in aqueous media, to our knowledge for the first time. This study developed a lead ion specific sensor by functionalizing the surface of hexagonal and triangular gold nanoparticles with DTT. Notably, the developed sensor exhibited great sensitivity for detection of lead ions over a wide concentration range and among various metal ions. The possible mechanism for the sensing action is also discussed, and it is proposed that unique corona formation around the DTT functionalized anisotropic GNP is attributed to the difference in the surface energies and hence different extent of surface functionalization of the corners and edges of the anisotropic GNP. Research and development of anisotropic nanoparticles based sensors is mainly focused on the nanorods of gold and silver metals. But, we believe that the use of other anisotropic nanoparticles of these metals with lower sphericity would broaden the scope and applicability of the sensors.

## ■ ASSOCIATED CONTENT

### ● Supporting Information

UV-vis spectrum and inset TEM image of unmodified spherical GNP; optimization of DTT concentration for surface functionalization of anisotropic GNP; zeta potential of the synthesized anisotropic GNP before and after surface functionalization with DTT; effect of contact time on the hydrodynamic radius of the DTT-functionalized anisotropic GNP; image of the change in the color of the DTT-modified anisotropic GNP with time and concentration of lead ions; effect of equilibration time on the change in absorption intensity of DTT-functionalized spherical GNP in the presence of lead ions; effect of equilibration time on the change in absorption intensity at different DTT functionalized anisotropic GNP concentration in the presence of lead ions; SPR shift at 880 nm at different lead ion concentrations; physicochemical properties of the tap water of Mandi, India; colorimetric assay performed on the tap water samples, spiked with different concentrations of  $\text{Pb}^{2+}$ . This material is available free of charge via the Internet at <http://pubs.acs.org>.

## ■ AUTHOR INFORMATION

### Corresponding Authors

\*E-mail: [charudwived@gmail.com](mailto:charudwived@gmail.com).

\*E-mail: [chayan@iitmandi.ac.in](mailto:chayan@iitmandi.ac.in). Tel.: +91 1905237917. Fax: +91 1905 237942

### Notes

The authors declare no competing financial interest.

## ■ ACKNOWLEDGMENTS

The authors acknowledge home institute (IIT Mandi) and Department of science & Technology India (Project SR/FT/CS-152/2011) for all the financial support. The authors acknowledge Mr. Abhishek Sharma, IIT Mandi, for his help in TEM measurement.

## ■ REFERENCES

(1) Yoosaf, K.; Ipe, B. I.; Suresh, C. H.; Thomas, K. G. In Situ Synthesis of Metal Nanoparticles and Selective Naked-Eye Detection of Lead Ions from Aqueous Media. *J. Phys. Chem. C* **2007**, *111*, 12839–12847.

(2) Borah, K.; Bhuyan, B.; Sarma, H. Lead, Arsenic, Fluoride, and Iron Contamination of Drinking Water in the Tea Garden Belt of Darrang District, Assam, India. *Environ. Monit. Assess.* **2010**, *169*, 347–352.

(3) Edwards, M. Fetal Death and Reduced Birth Rates Associated with Exposure to Lead-Contaminated Drinking Water. *Environ. Sci. Technol.* **2013**, *48*, 739–746.

(4) Tong, S.; Schirnding, Y. E. V.; Prapamontol, T. Environmental Lead Exposure: A Public Health Problem of Global Dimensions. *Bull. W. H. O.* **2000**, *78*, 1068–1077.

(5) Schwartz, J. Low-Level Lead Exposure and Children's IQ: A Metaanalysis and Search for a Threshold. *Environ. Res.* **1994**, *65*, 42–55.

(6) Soares, F.; Farina, M.; Santos, F.; Souza, D.; Rocha, J.; Nogueira, C. Interaction between Metals and Chelating Agents Affects Glutamate Binding on Brain Synaptic Membranes. *Neurochem. Res.* **2003**, *28*, 1859–1865.

(7) Ferhan, A. R.; Guo, L.; Zhou, X.; Chen, P.; Hong, S.; Kim, D.-H. Solid-Phase Colorimetric Sensor Based on Gold Nanoparticle-Loaded Polymer Brushes: Lead Detection as a Case Study. *Anal. Chem.* **2013**, *85*, 4094–4099.

(8) Li, J.; Lu, Y. A Highly Sensitive and Selective Catalytic DNA Biosensor for Lead Ions. *J. Am. Chem. Soc.* **2000**, *122*, 10466–10467.

(9) Godwin, H. A. The Biological Chemistry of Lead. *Curr. Opin. Chem. Biol.* **2001**, *5*, 223–227.

(10) Lu, Y. New Transition-Metal-Dependent Dnzymes as Efficient Endonucleases and as Selective Metal Biosensors. *Chem.—Eur. J.* **2002**, *8*, 4588–4596.

(11) Zhao, W.; Chiunan, W.; Lam, J. C. F.; Brook, M. A.; Li, Y. Simple and Rapid Colorimetric Enzyme Sensing Assays Using Non-Crosslinking Gold Nanoparticle Aggregation. *Chem. Commun.* **2007**, 3729–3731.

(12) Shiraiishi, Y.; Tanaka, K.; Hirai, T. Colorimetric Sensing of Cu(II) in Aqueous Media with a Spiropyran Derivative Via a Oxidative Dehydrogenation Mechanism. *ACS Appl. Mater. Interfaces* **2013**, *5*, 3456–3463.

(13) Huang, C.-C.; Chang, H.-T. Parameters for Selective Colorimetric Sensing of Mercury(II) in Aqueous Solutions Using Mercaptopropionic Acid-Modified Gold Nanoparticles. *Chem. Commun.* **2007**, 1215–1217.

(14) Jain, P.; Huang, X.; El-Sayed, I.; El-Sayed, M. Review of Some Interesting Surface Plasmon Resonance-Enhanced Properties of Noble Metal Nanoparticles and Their Applications to Biosystems. *Plasmonics* **2007**, *2*, 107–118.

(15) Chai, F.; Wang, C.; Wang, T.; Li, L.; Su, Z. Colorimetric Detection of  $\text{Pb}^{2+}$  Using Glutathione Functionalized Gold Nanoparticles. *ACS Appl. Mater. Interfaces* **2010**, *2*, 1466–1470.

(16) Si, S.; Raula, M.; Paira, T. K.; Mandal, T. K. Reversible Self-Assembly of Carboxylated Peptide-Functionalized Gold Nanoparticles Driven by Metal-Ion Coordination. *ChemPhysChem* **2008**, *9*, 1578–1584.

(17) Zheng, L.; Apps, J. A.; Zhang, Y.; Xu, T.; Birkholzer, J. T. On Mobilization of Lead and Arsenic in Groundwater in Response to  $\text{CO}_2$  Leakage from Deep Geological Storage. *Chem. Geol.* **2009**, *268*, 281–297.

(18) Liu, J.; Lu, Y. Optimization of a  $\text{Pb}^{2+}$ -Directed Gold Nanoparticle/Dnzyme Assembly and Its Application as a Colorimetric Biosensor for  $\text{Pb}^{2+}$ . *Chem. Mater.* **2004**, *16*, 3231–3238.

(19) Liu, J.; Lu, Y. A Colorimetric Lead Biosensor Using Dnzyme-Directed Assembly of Gold Nanoparticles. *J. Am. Chem. Soc.* **2003**, *125*, 6642–6643.

(20) Hui, W.; Bingling, L.; Jing, L.; Shaojun, D.; Erkang, W. Dnzyme-Based Colorimetric Sensing of Lead ( $\text{Pb}^{2+}$ ) Using Unmodified Gold Nanoparticle Probes. *Nanotechnology* **2008**, *19*, 095501.

(21) Li, N.; Zhao, P.; Astruc, D. Anisotropic Gold Nanoparticles: Synthesis, Properties, Applications, and Toxicity. *Angew. Chem., Int. Ed.* **2014**, *53*, 1756–1789.

(22) Durgadas, C. V.; Lakshmi, V. N.; Sharma, C. P.; Sreenivasan, K. Sensing of Lead Ions Using Glutathione Mediated End to End Assembled Gold Nanorod Chains. *Sens. Actuators, B* **2011**, *156*, 791–797.

(23) Chen, G.; Jin, Y.; Wang, L.; Deng, J.; Zhang, C. Gold Nanorods-Based FRET Assay for Ultrasensitive Detection of Hg<sup>2+</sup>. *Chem. Commun.* **2011**, *47*, 12500–12502.

(24) Murphy, C. J.; Gole, A. M.; Hunyadi, S. E.; Stone, J. W.; Sisco, P. N.; Alkilany, A.; Kinard, B. E.; Hankins, P. Chemical Sensing and Imaging with Metallic Nanorods. *Chem. Commun.* **2008**, 544–557.

(25) Hong, S.; Choi, Y.; Park, S. Shape Control of Ag Shell Growth on Au Nanodisks. *Chem. Mater.* **2011**, *23*, 5375–5378.

(26) Bai, X.; Zheng, L.; Li, N.; Dong, B.; Liu, H. Synthesis and Characterization of Microscale Gold Nanoplates Using Langmuir Monolayers of Long-Chain Ionic Liquid. *Crys. Growth Des.* **2008**, *8*, 3840–3846.

(27) Krężel, A.; Leśniak, W.; Jeżowska-Bojczuk, M.; Mlynarz, P.; Brasuń, J.; Kozłowski, H.; Bał, W. Coordination of Heavy Metals by Dithiothreitol, a Commonly Used Thiol Group Protectant. *J. Inorg. Biochem.* **2001**, *84*, 77–88.

(28) Kuo, C.-H.; Chiang, T.-F.; Chen, L.-J.; Huang, M. H. Synthesis of Highly Faceted Pentagonal- and Hexagonal-Shaped Gold Nanoparticles with Controlled Sizes by Sodium Dodecyl Sulfate. *Langmuir* **2004**, *20*, 7820–7824.

(29) Millstone, J. E.; Park, S.; Shuford, K. L.; Qin, L.; Schatz, G. C.; Mirkin, C. A. Observation of a Quadrupole Plasmon Mode for a Colloidal Solution of Gold Nanoprisms. *J. Am. Chem. Soc.* **2005**, *127*, 5312–5313.

(30) Jones, M. R.; Macfarlane, R. J.; Prigodich, A. E.; Patel, P. C.; Mirkin, C. A. Nanoparticle Shape Anisotropy Dictates the Collective Behavior of Surface-Bound Ligands. *J. Am. Chem. Soc.* **2011**, *133*, 18865–18869.